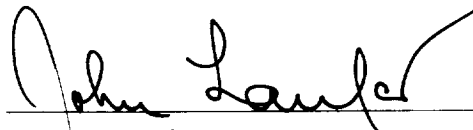


Technical Report No. 32-421

*Numerical Techniques for the Solution of the
Complete Bhatnagar–Gross–Krook Kinetic
Equation for Plane Shock Waves*

M. T. Chahine



J. Laufer, Chief
Fluid Physics Section

JET PROPULSION LABORATORY
CALIFORNIA INSTITUTE OF TECHNOLOGY
PASADENA, CALIFORNIA

June 3, 1963

Copyright © 1963
Jet Propulsion Laboratory
California Institute of Technology

Prepared Under Contract No. NAS 7-100
National Aeronautics & Space Administration

CONTENTS

I. Introduction	1
II. General Concept	2
III. Solution of the Navier-Stokes Equations	3
IV. Solution of the B-G-K Equations	5
A. First Iteration	5
B. Further Iterations	7
V. Numerical Evaluation of the Distribution Function	8
VI. Conclusion	9
Nomenclature	10
References	11

ABSTRACT

Details of the computational techniques are presented for the solution of the structure of normal plane shock waves in the Bhatnagar-Gross-Krook kinetic model.

I. INTRODUCTION

The structure of normal plane shock waves in a monatomic gas, using the Bhatnagar-Gross-Krook (B-G-K) collision model in an iteration scheme starting from the Navier-Stokes solution, has been the subject of Ref. 1 and 2. These works, however, do not include any discussion of the computational techniques employed in programming the iteration procedure on the IBM 7090, an elaborate task which, at the end, proved to be most rewarding.

The principal object of this Report is to lay out a process for an iterative solution of the B-G-K kinetic equation. But, since a process may be well adapted to one machine and poorly adapted to another, this Report will be mainly concerned with first principles from which

to construct such rules as seem to conform best to the idiosyncrasies of the particular machine in use.

A statement of the mathematical principles that are of assistance in the design of the computational program is presented in Section II, followed by a general discussion of the Navier-Stokes numerical solution in Section III. In Section IV the basic iterative equations are simplified in order to be suitable for machine computation, and in Section V the distribution function within the shock wave is examined. Finally, in Section VI the numerical results of Ref. 1 and 2 are used to gain some insight into the effect of Mach number and estimate of errors on the rate of convergence.

II. GENERAL CONCEPT

In Ref. 1 and 2 the structure of shock waves is discussed on the basis of the Bhatnagar-Gross-Krook kinetic equation written in the form

$$v_x \frac{\partial f}{\partial x} = \Lambda_1 A n [F - f] \quad (1)$$

with

$$A = mR \frac{T(x)}{\mu(T)} \quad (2)$$

$$x = \frac{\bar{x}}{\Lambda_1}$$

where $f = f(\mathbf{v}, x)$ is the velocity distribution function along the direction of motion x of the gas perpendicular to the shock wave; $1/\Lambda n$ is the relaxation time which depends on the local state of the gas; Λ_1 is the Maxwellian mean free path ahead of the shock; and $F(\mathbf{v}, x)$ is the local Maxwellian distribution function

$$F(\mathbf{v}, x) = \frac{n(x)}{[2\pi RT(x)]^{3/2}} \exp - \left\{ \frac{[\mathbf{v} - \mathbf{u}(x)]^2}{2RT(x)} \right\} \quad (3)$$

corresponding at every point to the average number density

$$n(x) = \int_{-\infty}^{+\infty} f(\mathbf{v}, x) d\mathbf{v} \quad (4a)$$

velocity

$$u(x) n(x) = \int_{-\infty}^{+\infty} v_x f(\mathbf{v}, x) d\mathbf{v} \quad (4b)$$

and temperature

$$3Rn(x) T(x) = \int_{-\infty}^{+\infty} [\mathbf{v} - \mathbf{u}(x)]^2 f(\mathbf{v}, x) d\mathbf{v}$$

$$= -u^2(x) n(x) + \int_{-\infty}^{+\infty} (\mathbf{v} \cdot \mathbf{v}) f(\mathbf{v}, x) d\mathbf{v} \quad (4c)$$

To this we must add the condition that as $x \rightarrow \infty$, the distribution function f approaches the Maxwellian functions

$$f(\mathbf{v}, -\infty) = F_1 \quad \text{and} \quad f(\mathbf{v}, +\infty) = F_2 \quad (5)$$

the parameters n_1, u_1, T_1 and n_2, u_2, T_2 defining F_1 and F_2 being related by the Rankine-Hugoniot conditions.

Formal integration of Eq. (1) for $v_x \leq 0$ respectively, subject to the boundary conditions of Eq. (5), yields

$$f_-(v_x < 0, v_y, v_z, x) = \int_{+\infty}^x \frac{An}{v_x} F \exp - \left\{ \int_{x'}^x \frac{An}{v_x} dx'' \right\} dx' \quad (6)$$

and

$$f_+(v_x > 0, v_y, v_z, x) = \int_{-\infty}^x \frac{An}{v_x} F \exp - \left\{ \int_{x'}^x \frac{An}{v_x} dx'' \right\} dx'$$

Equations (4a)–(4c) together with Eq. (6) form a system of four equations with four unknowns, f, n, u , and T . The solution of this system of equations can formally be obtained by constructing a sequence of functions, $n^j(x)$, $u^j(x)$ and $T^j(x)$. This process of iteration is seldom useful for carrying the integration unless a good approximation is available to use as a first approximation, $n^0(x)$, $u^0(x)$ and $T^0(x)$ in the right-hand side of Eq. 4 and 6; otherwise the convergence of the successive functions u^j, n^j and T^j to the solution of the equation becomes slow. Reference 2 shows that the solution of the Navier-Stokes equation across the shock is quite adequate to use as initial input.

III. SOLUTION OF THE NAVIER-STOKES EQUATIONS

The one-dimensional Navier-Stokes equations for a monatomic gas in steady flow are

$$\frac{d}{d\bar{x}}(nmu) = 0$$

$$\frac{d}{d\bar{x}} \left(nmu^2 + nmRT - \frac{4}{3} \mu \frac{du}{d\bar{x}} \right) = 0 \quad (7)$$

$$\frac{d}{d\bar{x}} \left[nmu \left(\frac{3}{2} RT + \frac{1}{2} u^2 \right) + u \left(nmRT - \frac{4}{3} \mu \frac{du}{d\bar{x}} \right) - K \frac{dT}{d\bar{x}} \right] = 0$$

The methods suggested in Ref. 3, 4, and 5 for the solution of these equations require the reduction of Eq. (7) to the form¹

$$\frac{dt}{dw} = \frac{2}{15} Pr \frac{[6(t+w) + B(1-w^2)][5+Bw]}{2(t+w) - B(1-w^2)} \quad (8a)$$

$$\frac{dw}{dx} = \frac{1}{4} \sqrt{\frac{15\pi}{2}} M_1 \frac{2(t+w) - B(1-w^2)}{(5+Bw)(\mu'/\mu_1)} \quad (8b)$$

$$B = \frac{15(M_1^2 - 1)}{3 + 5M_1^2} \quad (9a)$$

$$Pr = \mu \frac{C_p}{K} \quad \text{and} \quad 3\mu + 2\mu' = 0 \quad (9b)$$

where t and w are normalized temperature and velocity variables related to the actual nondimensional values by Eq. (10a) and (10b). The nature of Eq. (8) is such that in the $t-w$ plane t and w vary from $w_1 = 1$ and $t_1 = -1$ (nodal point) to $w_2 = -1$ and $t_2 = +1$ (saddle point) for the whole range of the shock profile

The present computations were carried out on the IBM 7090 starting from the saddle-point singularity (downstream from the shock) and following the standard textbook method of step-by-step integration of the direction field.

Input: For a given Mach number M_1 , the initial slope dt/dw at the saddle point is determined from Eq. (8a) by

l'Hospital's rule. For the purpose of this iteration scheme it is necessary to use a fine increment of $\Delta w = 0.002$. The Prandtl number $Pr = 1$ remains constant throughout the shock, and the viscosity μ is defined as a function of the temperature.

Procedure: First, t as a function of w is calculated (Eq. 9); then the profile in terms of x is obtained by taking the origin of the x axis at the point of maximum velocity gradient dw/dx_{\max} , and by integrating Eq. (8b) starting from $x = 0$ and proceeding upstream to $x_{(i)}$ and downstream to $x_{(1)}$. The effect of round-off errors in the early intervals of this integration builds up rather fast, so that it is necessary to keep a large number of guarding figures and work to eight decimals. To achieve this accuracy at high Mach numbers it is necessary to apply a fourth-order Runge-Kutta integration formula.

Output: The following flow parameters were calculated, tabulated, and stored in the memory of the computer (superscript 0 refers to the Navier-Stokes solution, and subscript 1 refers to the upstream conditions):

$$\Theta^0(x) = \frac{T^0(x)}{T_1} = \frac{15 - B^2 + 2Bt}{15 - B^2 - 2B} \quad (10a)$$

$$U^0(x) = \frac{u^0(x)}{u_1} = \frac{5 + Bw}{5 + B} \quad (10b)$$

$$N^0(x) = \frac{n^0(x)}{n_1} = \frac{1}{u^0(x)/u_1} \quad (10c)$$

$$S^0(x) = \sqrt{\frac{5}{6}} M_1 \frac{U^0(x)}{\sqrt{\Theta^0(x)}} = \frac{u^0(x)}{\sqrt{2RT^0(x)}} \quad (10d)$$

$$L^0(x) = \frac{\Lambda^0(x)}{\Lambda_1} = \frac{\mu^0(T)/\mu_1}{N^0(x) \sqrt{\Theta^0(x)}} \quad (10e)$$

and

$$\xi_1^0 = x_{(i)} < 0; \quad \xi_2^0 = x_{(1)} > 0$$

Following the tabulation of this set of five parameters, an appropriate interpolation formula is chosen. Here, the use of a third-order polynomial is convenient in accordance with the monotonic nature of Eq. (10). For extrapolation it is useful to put a close in the program requiring the flow parameters to be equal to their respective con-

¹See Ref. 5, Appendix B.

stant upstream values for $x < \xi_1^0$, and downstream values for $x > \xi_2^0$.

The program also calculated, stored, and retained the following shock constants:

$$S_1 = \sqrt{\frac{5}{6}} M_1 \quad (11a)$$

$$S_2 = \sqrt{\frac{5}{6}} \frac{M_1^2 + 3}{5M_1^2 - 1} \quad (11b)$$

$$N_2 = \frac{n_2}{n_1} = \frac{4 M_1^2}{M_1^2 + 3} \quad (11c)$$

$$\Theta_2 = \frac{T_2}{T_1} = \frac{5M_1^2 + 14 M_1^2 - 3}{16 M_1^2} \quad (11d)$$

$$L_2 = \frac{\Lambda_2}{\Lambda_1} = \frac{\mu_2/\mu_1}{N_2 \sqrt{\Theta_2}} \quad (11e)$$

The average time required to solve and compile this portion of the program is less than one minute.

IV. SOLUTION OF THE B-G-K EQUATIONS

The essence of the iteration procedure can be described very briefly. The B-G-K distribution function $f_{\pm}^1(\mathbf{v}, x)$ of Eq. (6) is first prescribed in terms of n^0 , u^0 and T^0 to read

$$f_{\pm}^1 = \int_{\pm\infty}^x \frac{A^0(x') n^0(x')}{v_x} F^0(\mathbf{v}, x') \exp - \left\{ \int_{x'}^x \frac{A^0(x'') n^0(x'')}{v_x} dx'' \right\} dx' \quad (12)$$

where

$$F^0(\mathbf{v}, x') = \frac{n^0(x')}{[2\pi RT^0(x')]^{3/2}} \exp - \left\{ \frac{[\mathbf{v} - \mathbf{u}^0(x')]^2}{2RT^0(x')} \right\}$$

then substituted into Eq. (4) to yield the new values of the moments $u^1(x)$, $n^1(x)$, $T^1(x)$, which in turn generate the next step in the iteration scheme

The processes and arguments by which $n^1(x)$, $u^1(x)$ and $T^1(x)$ are solved may be properly illustrated by considering as a specific but typical example the first moment $n^1(x)$

$$n^1(x) = \int_{-\infty}^{+\infty} \int_{-\infty}^{+\infty} \left[\int_{-\infty}^0 f_{-}^1 dv_x + \int_0^{+\infty} f_{+}^1 dv_x \right] dv_y dv_z \quad (13)$$

Equation (13) can be integrated immediately with respect to v_y and v_z and reduced to read

$$\begin{aligned} \frac{2n^1(x)}{n_1} &= \int_0^{+\infty} \int_x^{+\infty} \frac{N^0(x')}{L^0(x')} \frac{1}{\eta} \\ &\exp - \left\{ [\eta - S(x')]^2 + \frac{h^0(x', x)}{\eta} \right\} dx' d\eta \\ &+ \int_0^{+\infty} \int_{-\infty}^x \frac{N^0(x')}{L^0(x')} \frac{1}{\eta} \\ &\exp - \left\{ [\eta - S(x')]^2 + \frac{h^0(x', x)}{\eta} \right\} dx' d\eta \quad (14) \end{aligned}$$

where

$$S = \frac{u}{\sqrt{2RT}}$$

$$\eta = \frac{v_x}{\sqrt{2RT}}$$

$$L^0(x') = \frac{\mu^0/\mu_1}{N^0(x') [\Theta^0(x')]^{1/2}} \quad (15)$$

$$h^0(x', x) = \frac{\sqrt{\pi}}{2} [\Theta^0(x')]^{-1/2} \int_{x'}^x \frac{[\Theta^0(x'')]^{1/2}}{L^0(x'')} dx''$$

with x' and x denoting, respectively, the lower and upper limits of the integral with respect to x'' . Consequently,

$$\frac{h^0(x', x)}{\eta} \geq 0 \quad (16)$$

and the integrand is limited and does not change sign. Hence it can be shown analytically that the above function is always convergent.

A. First Iteration

The function $n^1(x)$ given in Eq. (15) involves a set of infinite limits which are impractical for rapid numerical calculations. It is possible, however, to adapt each term of this integral for machine computations by considering first the integrand over the path of integration $\eta = 0 \rightarrow \pm \infty$; for $h^0(x', x) \neq 0$ the part corresponding to large η furnishes a contribution which becomes smaller as η becomes larger. Thus the apparent advantage of this consists in the fact that a truncation of the path of integration with respect to η at a point where

$$\exp - \left\{ (\eta - S^0)^2 + \frac{h^0(x', x)}{\eta} \right\} \leq 10^{-32}$$

would leave the calculations with substantial accuracy. Second, the fact that Eq. (10a)-(10e) are tabulated constants equal to their respective Rankine-Hugoniot values for $-\infty < x' < \xi_1^0$ and $\xi_2^0 < x' < +\infty$ may be used to integrate Eq. (15) analytically with respect to x' over portions of the path, $\xi_1^0 \rightarrow -\infty$ and $\xi_2^0 \rightarrow +\infty$. However, when this integration is performed there will arise for $x > \xi_1^0$ and $x < \xi_2^0$ operations which cannot be handled by digital computations. Therefore, in order to satisfy Eq. (16) at all times, and thereby evade such operations, it is necessary to introduce a symbolic function $H(\alpha)$ defined by

$$\begin{aligned} H(\alpha) &= 1 & \alpha > 0 \\ &= 0 & \alpha < 0 \end{aligned} \quad (17)$$

Performance of these simplifications may be employed to advantage to develop the final expression of $n^1(x)$ into

$$\begin{aligned}
2N^1(x) = & H(\xi_2^0 - x) \int_0^{-\infty} \int_x^{\xi_1^0} \frac{N^0(x')}{L^0(x')} \frac{1}{\eta} \exp - \left\{ [\eta - S^0(x')]^2 + \frac{h^0(x', x)}{\eta} \right\} d\eta dx' \\
& - H(x - \xi_1^0) \int_0^{+\infty} \int_x^{\xi_1^0} \frac{N^0(x')}{L^0(x')} \frac{1}{\eta} \exp - \left\{ [\eta - S^0(x')]^2 + \frac{h^0(x', x)}{\eta} \right\} d\eta dx' \\
& - H(\xi_2^0 - x) \frac{\sqrt{\pi}}{2} N_2 \int_0^{-\infty} \exp - \left\{ (\eta - S_2)^2 + \frac{h^0(\xi_2^0, x)}{\eta} \right\} d\eta \\
& + H(x - \xi_1^0) \frac{\sqrt{\pi}}{2} \int_0^{+\infty} \exp - \left\{ (\eta - S_1)^2 + \frac{h^0(\xi_1^0, x)}{\eta} \right\} d\eta \\
& - H(x - \xi_2^0) \frac{\sqrt{\pi}}{2} N_2 \int_0^{-\infty} \exp - \{(\eta - S_2)^2\} d\eta \\
& + H(\xi_1^0 - x) \frac{\sqrt{\pi}}{2} \int_0^{+\infty} \exp - \{(\eta - S_1)^2\} d\eta
\end{aligned} \tag{18}$$

Similarly Eq. (4b) and (4c) become

$$\begin{aligned}
2U^1(x) N^1(x) = & H(\xi_2^0 - x) \int_0^{-\infty} \int_x^{\xi_1^0} \frac{U^0(x') N^0(x')}{L^0(x') S^0(x')} \exp - \left\{ [\eta - S^0(x')]^2 + \frac{h^0(x', x)}{\eta} \right\} d\eta dx' \\
& - H(x - \xi_1^0) \int_0^{+\infty} \int_x^{\xi_1^0} \frac{U^0(x') N^0(x')}{L^0(x') S^0(x')} \exp - \left\{ [\eta - S^0(x')]^2 + \frac{h^0(x', x)}{\eta} \right\} d\eta dx' \\
& - H(\xi_2^0 - x) \frac{\sqrt{\pi}}{2} \frac{1}{S_2} \int_0^{-\infty} \eta \exp - \left\{ (\eta - S_2)^2 + \frac{h^0(\xi_2^0, x)}{\eta} \right\} d\eta \\
& + H(x - \xi_1^0) \frac{\sqrt{\pi}}{2} \frac{1}{S_1} \int_0^{+\infty} \eta \exp - \left\{ (\eta - S_1)^2 + \frac{h^0(\xi_1^0, x)}{\eta} \right\} d\eta \\
& - H(x - \xi_2^0) \frac{\sqrt{\pi}}{2} \frac{1}{S_2} \int_0^{-\infty} \eta \exp - \{(\eta - S_2)^2\} d\eta \\
& + H(\xi_1^0 - x) \frac{\sqrt{\pi}}{2} \frac{1}{S_1} \int_0^{+\infty} \eta \exp - \{(\eta - S_1)^2\} d\eta
\end{aligned} \tag{19}$$

$$\begin{aligned}
3\Theta^1(x) N^1(x) = & H(\xi_2^0 - x) \int_0^{-\infty} \int_x^{\xi_1^0} \frac{\Theta^0(x') N^0(x')}{L^0(x')} \frac{\eta^2 + 1}{\eta} \exp - \left\{ [\eta - S^0(x')]^2 + \frac{h^0(x', x)}{\eta} \right\} d\eta dx' \\
& - H(x - \xi_1^0) \int_0^{+\infty} \int_x^{\xi_1^0} \frac{\Theta^0(x') N^0(x')}{L^0(x')} \frac{\eta^2 + 1}{\eta} \exp - \left\{ [\eta - S^0(x')]^2 + \frac{h^0(x', x)}{\eta} \right\} d\eta dx' \\
& - H(\xi_2^0 - x) \frac{\sqrt{\pi}}{2} \Theta_2 N_2 \int_0^{-\infty} (\eta^2 + 1) \exp - \left\{ (\eta - S_2)^2 + \frac{h^0(\xi_2^0, x)}{\eta} \right\} d\eta \\
& + H(x - \xi_1^0) \frac{\sqrt{\pi}}{2} \int_0^{+\infty} (\eta^2 + 1) \exp - \left\{ (\eta - S_1)^2 + \frac{h^0(\xi_1^0, x)}{\eta} \right\} d\eta \\
& - H(x - \xi_2^0) \frac{\sqrt{\pi}}{2} \Theta_2 N_2 \int_0^{-\infty} (\eta^2 + 1) \exp - \{(\eta - S_2)^2\} d\eta \\
& + H(\xi_1^0 - x) \frac{\sqrt{\pi}}{2} \int_0^{+\infty} (\eta^2 + 1) \exp - \{(\eta - S_1)^2\} d\eta \\
& - 2 N^1(x) [S_1 U^1(x)]^2
\end{aligned} \tag{20}$$

This may appear a rather elaborate form of Eq. (4) but, in fact, is quite convenient for numerical computations.

Input: As already mentioned, the tabulated and stored results of the Navier-Stokes solution constitute the input to the first iteration. The interval used is

$$\Delta\eta = 0.1$$

However, in order to keep the integration with respect to x' correct, in each interval, within the tolerance for round-off error, two sets of intervals are needed:

$$\begin{aligned}\Delta x' = \Delta x'' = 0.01 & \quad \text{for } |x - x'| \leq 0.1 \\ & = 0.1 \quad \text{for } |x - x'| > 0.1\end{aligned}$$

In the computations reported in Ref. (1) and (2), the equations were computed for 30 different values of x . For the first point the value of $x_{(1)} \approx \xi_2^0 > 0$ is taken with ten points between 0 and ξ_2^0 . The last $x_{(30)} < \xi_1^0 < 0$ is determined by trial and error until $\Theta^1(x) \approx U^1(x) \approx N^1(x) \rightarrow 1$ as $x \rightarrow x_{(30)}$.

Procedure: Equations (18), (19), and (20) are evaluated simultaneously for each value of x . The first and second terms are computed numerically using a Gaussian quadrature formula in each interval. A step-by-step integration is initiated by evaluating $h^0(x', x)$ at $x' = x + \Delta x'$, and the integrand is determined by interpolating the values of the other parameters at the required value of x' . The same procedure is repeated for the following values of $x' = x + k \Delta x'$; then a set of integrations with respect to η is carried out for the set of values of x' . Finally, interpolation with respect to x' is employed to integrate the functions with respect to x' . The evaluation of the third and fourth terms is reduced to a single integration with respect to η (Ref. 6) by evaluating separately $h^0(\xi_1^0, x)$ and $h^0(\xi_2^0, x)$ for all values of x .

From the behavior of the solution reported in Ref. (1) and (2), we note here that the integral for $x > 0$ (high density side of the shock) is very sensitive to the step size, to the accuracy of the initial Navier-Stokes solution, and to the effects of rounding-off errors, while the same thing cannot be said for $x < 0$ (low-density side).

The computational error introduced in evaluating Eq. (19) and (20) is less than $\pm 5 \times 10^{-3}$; however, due to the predominant existence of $1/\eta$ in the integrand of Eq. (18), the computational error introduced in $N(x)$ is relatively bigger.

The reason behind computing and tabulating both $N(x)$ and $U(x)$ is that the conservation of mass in the present iterative solution is attained only after a certain number of iterations; thus $u^1(x) n^1(x)$ is not identically equal to $u_1 n_1$ and $u_2 n_2$ except at $x = \pm \infty$.

Output: The tabulated flow parameters of the Navier-Stokes solutions are now replaced by their corresponding values from the first iteration, namely

$$\Theta^1(x), U^1(x), N^1(x), S^1(x), L^1(x)$$

$$\xi_1^1 = x_{(1)} < 0 \text{ and } \xi_2^1 = x_{(30)} > 0$$

The average time required to solve and compile this portion of the program is around 90 seconds for each value of x .

B. Further Iterations

The succeeding iterations are performed in a manner similar to the one explained in Section IV-A simply by replacing the j superscript by $j + 1$ and by using as input the output of the j th iteration. To pursue the iteration further requires a delicate study of the total error regarded as a build-up from round-off and truncation errors. The first can be estimated in terms of the precision of the tabulated results of the previous iteration, and the latter depends on the formulas used in the program. This suggests that at some stage the residual errors and the generated errors might be of such magnitude that continuation of the process is unprofitable. In any case, in estimating these errors we should suppose that the equations to be solved are themselves exact.

The time required to compute and compile each iteration on the IBM 7090 is estimated to be $10(\xi_2^j - \xi_1^j)$ seconds for each value of x .

V. NUMERICAL EVALUATION OF THE DISTRIBUTION FUNCTION

The numerical process discussed in Section IV, together with the output of the last accurate iteration, say the j th, may be employed to solve for the distribution function $f_{\mp}(\mathbf{v}, x)$ given by Eq. (6).

Since the integrands of Eq. (6) do not change sign along their respective range of integration, it can be easily shown that both

$$f_{\mp}(\mathbf{v}, x) \geq 0 \quad (21)$$

In the present calculations we are interested in evaluating Eq. (6) in the range of $\xi_1^j < x < \xi_2^j$. For x outside this range, Eq. (6) behaves like a Maxwellian.

In order to reduce Eq. (6) to a form compatible with the tabulated results of the j th iteration, and suitable for machine calculation, we make use of Eq. (11) and (17) to get

$$\begin{aligned} & \frac{f_{-}(v_x < 0, v_y, v_z, x)}{n_1 (2\pi RT_1)^{-3/2}} \\ &= \frac{\sqrt{\pi}}{2} \int_{\xi_1^j}^x \frac{N^j(x')}{L^j(x') \Theta^j(x')} \frac{1}{q_x} \exp - \left\{ \frac{[q_x - S^j(x') \sqrt{\Theta^j(x')}]^2 + q_y^2 + q_z^2}{\Theta^j(x')} + \frac{J^j(x', x)}{q_x} \right\} dx' \\ &+ \frac{N_2}{(\Theta_2)^{3/2}} \exp - \left\{ \frac{[q_x - S_2 \sqrt{\Theta_2}]^2 + q_y^2 + q_z^2}{\Theta_2} + \frac{J^j(\xi_2^j, x)}{q_x} \right\} \end{aligned} \quad (22)$$

and

$$\begin{aligned} & \frac{f_{+}(v_x > 0, v_y, v_z, x)}{n_1 (2\pi RT_1)^{3/2}} \\ &= \frac{\sqrt{\pi}}{2} \int_{\xi_1^j}^x \frac{N^j(x')}{L^j(x') \Theta^j(x')} \frac{1}{q_x} \exp - \left\{ \frac{[q_x - S^j(x') \sqrt{\Theta^j(x')}]^2 + q_y^2 + q_z^2}{\Theta^j(x')} + \frac{J^j(x', x)}{q_x} \right\} dx' \\ &+ \exp - \left\{ (q_x - S_1)^2 + q_y^2 + q_z^2 + \frac{J^j(\xi_1^j, x)}{q_x} \right\} \end{aligned}$$

where

$$\mathbf{q} = \frac{\mathbf{v}}{\sqrt{2RT_1}}, \quad \xi_1^j < x < \xi_2^j$$

and

$$J^j(x', x) = \frac{\sqrt{\pi}}{2} \int_{x'}^x \frac{\sqrt{\Theta^j(x'')}}{L^j(x'')} dx''$$

In evaluating Eq. (22) it is necessary to specify certain values of x within the shock profile, and compute f for a wide range of q_x , q_y , and q_z . From the preliminary results (not yet reported) conducted in connection with Ref. (1) and (2), it can be noted that, for an arbitrary value of $x = l$, the major variation of f with respect to q_x is covered by the range

$$-5 < \left(\frac{v_x - u}{\sqrt{2RT}} = \frac{q_x - S\sqrt{\Theta(x)}}{\sqrt{\Theta(x)}} \right)_{x=l} < +5 \quad (23)$$

VI. CONCLUSION

The fact that the present iterative process theoretically converges to a given limit does not of itself imply that the results of the digital computations will approach this limit. The present iterative solution is necessarily a finite numerical process in which the concept of formal convergence hardly plays any role, though it is involved in the analytical arguments by which the process is established. Therefore, any conclusion about the convergence should not be made without taking into account the error introduced from the previous steps. In this connection the rate of convergence of the present work can best be judged by the rate with which Eq. (14) approaches one, $u^j(x) n^j(x)/u_1 n_1 \rightarrow 1$, throughout the shock.

From the results reported in Ref. (1) and (2) for this type of initial input, it is seen that the rate of convergence

is a function of M_1 , the Mach number ahead of the shock. At low Mach numbers, $M_1 = 1.5$, one iteration is enough to reproduce the Navier-Stokes solution which is known to be accurate in this range. In the intermediate range, $M_1 = 3.0$, the rate of convergence is slower, and the iteration process is very sensitive to all the technical aspects of the program such as step size, interpolation formulas, truncation, etc. Consequently the range of low Mach numbers, $M_1 = 1.5$, is recommended to check the program for any mistakes or gross errors, while the intermediate range, $M_1 = 3.0$, is most adequate to judge the wisdom of the assumptions involved in the numerical process. In the range of high Mach numbers, $M_1 = 5.0$ and 10.0, the process converges relatively faster with the low-density side, $x < 0$, being less sensitive than the high-density side.

NOMENCLATURE

A	parameter in the B-G-K collision model, see Eq. (2)	t	normalized temperature, see Eq. (10a)
B	constant, see Eq. (9a)	U	velocity ratio, see Eq. (10b)
C_p	specific heat at constant pressure	u	mass velocity along the x-axis
F	Maxwellian distribution	v	molecular velocity (v_x, v_y, v_z)
f	molecular velocity distribution function	w	normalized mass velocity, see Eq. (10b)
H	symbolic function, see Eq. (17)	\bar{x}	physical axis along the direction of flow
h	mathematical expression, see Eq. (15)	x	nondimensional physical axis, see Eq. (2)
J	mathematical expression, see Eq. (22)	η	molecular velocity, see Eq. (15)
K	heat-conduction coefficient	Θ	temperature ratio, see Eq. (10a)
L	Mean free path ratio, see Eq. (10c)	Λ	$= \sqrt{\frac{5\pi}{6}} \frac{M}{nm\mu} =$ Maxwellian mean free path
M	Mach number	μ	viscosity
m	molecular mass		
N	density ratio, see Eq. (10c)	Superscript	
n	number density	⁰	initial input
Pr	Prandtl number	₁	first iteration
q	molecular velocity (q_x, q_y, q_z), see Eq. (22)	_j	jth iteration
R	Boltzmann gas constant	Subscript	
S	speed ratio, see Eq. (10d)	₁	conditions at $-\infty$ (ahead of the shock)
T	temperature	₂	conditions at $+\infty$ (behind the shock)

REFERENCES

1. Chahine, M. T., *The Structure of Strong Shock Waves in the Krook Collision Model*, Technical Report No. 32-327, Jet Propulsion Laboratory, Pasadena, California. Also in *Proceedings of the Third International Symposium on Rarefied Gas Dynamics*, Paris, June 1962, J. Laurmann, Editor, Academic Press (in press).
2. Liepmann, H. W., R. Narasimha, and M. T. Chahine, *The Structure of Plane Shock Layers*, Technical Report No. 32-342, Jet Propulsion Laboratory, Pasadena, California. Also in *The Physics of Fluids*, Vol. 5, No. 11, November 1962.
3. Gilbarg, D., and D. Paolucci, "The Structure of Shock Waves in the Continuum Theory of Fluids," *Journal of Rational Mechanics and Analysis*, Vol. 2, No. 4, 1953, pp. 617-642.
4. Grad, H., "The Profile of a Steady Plane Shock Wave," *Communications on Pure and Applied Mathematics*, Vol. V, No. 3, August 1962, pp. 257-300.
5. Sherman, F. S., *A Low-Density Wind-Tunnel Study of Shock-Wave Structure and Relaxation Phenomena in Gases*, NASA TN 3298, July 1955.
6. Chahine, M. T., and R. Narasimha, *Evaluation of the Integral*

$$\int_0^{\infty} v^n \exp \left\{ -(v-u)^2 - \frac{x}{v} \right\} dv,$$

Technical Report No. 32-459, Jet Propulsion Laboratory, Pasadena, California (in preparation).

ACKNOWLEDGMENT

The author is indebted to Mr. Sherwin Levy for programming this problem and for valuable discussions on the techniques of numerical computations.

